



Platinum-encapsulated zeolitically microcapsular catalyst for one-pot dynamic kinetic resolution of phenylethylamine

Jing Shi, Xiang Li, Quanrui Wang, Yahong Zhang*, Yi Tang*

Department of Chemistry, Shanghai Key Laboratory of Molecular Catalysis and Innovative Materials, Institute of Catalysis, and Laboratory of Advanced Material, Fudan University, Shanghai 200433, PR China

ARTICLE INFO

Article history:

Received 17 November 2011
Revised 12 March 2012
Accepted 15 April 2012
Available online 16 May 2012

Keywords:

Zeolitic microcapsule
Multifunction catalyst
Isolation of active sites
Phenylethylamine
Dynamic kinetic resolution

ABSTRACT

The platinum-encapsulated zeolitically microcapsular catalyst, associated with the immobilized *Candida antarctica* lipase B (Novozyme®435), is successfully employed in the dynamic kinetic resolution of phenylethylamine. A conversion of 80% and a selectivity of 95% are achieved, and negligible loss of activity is detected even after reaction of 5 runs. It is found that the existence of the silicalite-1 shell not only effectively prevents the deactivation of both enzyme and Pt by isolating them in different regions of reaction system, but also significantly reduces the formation of by-products on the Pt nanoparticles within the protected space of zeolitic microcapsule. Such features of zeolitic shell should further promote the designing of various catalysts for multistep reaction network.

© 2012 Elsevier Inc. All rights reserved.

1. Introduction

During the last decades, microcapsule has been developed to be an attractive material used for various applications in pharmaceutical, cosmetic, food, textile, adhesive, agricultural industries and catalytic domains [1–7]. Up to now, the structure of the capsule has been evolved from the zero-dimensional solid spheres and one-dimensional wires, rods or belts (identified as the first generation of one-level structure) to the second generation with core-shell construction as the two-level structural materials and then the third generation with multilevel interiors including diverse complex architectures such as the multishell spheres, the multichamber spheres, the multiwalled tubes and the multichannel tubes [8–11]. In terms of the composition of the microcapsule, it mainly covers the inorganic compounds (carbon, silicon and calcium), organic compounds or inorganic/organic hybrid substances as well as the organometallic species [12–17]. Among them, the inorganically zeolitic microcapsule (ZMC) has attracted much attention due to the unique characteristics provided by its special configuration, such as the confined space effect, the high-thermal stability and the molecular sieving effect [18–20]. The encapsulation of catalytic active species into ZMC has been highlighted by using them in the practical reactions of alcohol oxidation, Heck

coupling reaction, direct synthesis reactions of middle isoparaffins and dimethyl ether (DME) from syngas and so on [21–24]. And it has been proved that the zeolitic shell can not only protect the active species from poisoning and leaching outside during the reaction but also contribute a high spatial selectivity and shape selectivity for the products with different molecular sizes.

Nowadays, the optically pure enantiomers are of great significance in chiral chemistry, agricultural chemistry and pharmaceutical chemistry [25–27]. A variety of methods have been used to obtain pure enantiomers, such as the kinetic resolution (KR), the asymmetric synthesis and the chiral chromatography separation [28–30]. The KR process using enzyme as an acylation catalyst has grown to be an important and appealing method owing to its high efficiency and moderate condition. However, the theoretical yield limit of 50% remains a main drawback for this process [31]. An effective strategy to overcome this problem is dynamic kinetic resolution (DKR) by combining the KR with the racemization of enantiomers in a one-pot system [31]. By surpassing the limitation of KR, DKR is theoretically possible to obtain 100% yield of the pure enantiomers from a racemic mixture. Various catalysts, such as the metal nanoparticles, the solid acidic materials and the organometallic complexes, have been explored to catalyze the racemization reaction under a defined reaction condition [32,33]. The metal catalyzed racemization mainly relies on the reversible hydrogen-transfer process and/or the hydrogenation and dehydrogenation course [34,35], but its development in this field is still a challenge. Platinum, known as an efficient catalyst for hydrogenation and dehydrogenation procedure [36], has been used for racemization

* Corresponding authors. Address: Department of Chemistry, Fudan University, No. 220, Handan Road, Shanghai 200433, PR China. Fax: +86 21 65641740.

E-mail addresses: zhangyh@fudan.edu.cn (Y. Zhang), yitang@fudan.edu.cn (Y. Tang).

of 1,1'-binaphthyl ever since 1982 by Pincock [37]. However, only a few reports were published for further application of platinum in DKR process [38], probably due to its interaction with the enzyme [39,40]. The metal could act as an inhibitor for enzyme in the acylation reaction, and the interference of enzyme with metal may also lead to poor racemization on the latter, as was pointed out by Martín-Matute and Backväll [40].

Herein, the ZMC with encapsulated platinum nanoparticles and an intact thin shell of silicalite-1 (denoted as intact-Pt@S1) is employed as racemization catalyst in the DKR of phenylethylamine (PEA) for the first time. Thanks to the protection of the zeolitic shell, this emerged catalyst associated with enzyme displays high selectivity and activity for DKR of PEA. Through the comparison with the data obtained from the heavily grinded broken capsules (denoted as broken-Pt@S1), the positive effects of the intact zeolitic shell on the one-pot DKR of PEA are well confirmed.

2. Experimental

2.1. Materials

Polydiallyldimethylammonium chloride (PDDA, Mw = 200,000, 10 wt% in water), poly (sodium 4-styrene sulfonate) (PSS, Mw = 70,000), 3-amino-propyltriethoxysilane (APS) and Novozyme[®] 435 (*Candida antarctica* lipase B immobilized onto acrylic resin) were purchased from Aldrich. \pm -1-PEA (rac-PEA, 98%), S-1-PEA (98%) and R-1-PEA (98%) were obtained from Alfa Aesar. Decane (>99%) was achieved from Acros. Vinyl octanoate (98%) was purchased from ABCR. Acetaldehyde (99.5%) was obtained from Adamas. H₂PtCl₆·6H₂O and octanoic acid were supplied by Sinopharm Chemical Reagent Company. KBH₄ (94 wt%), tetrapropylammonium hydroxide (TPAOH, 25 wt% in water), tetrapropyl ammonium bromide (TPABr) and tetraethoxy-orthosilane (TEOS) were obtained from Shanghai Chemical Reagent Company. Toluene (>99%) and sodium hydroxide (NaOH) were achieved from Shanghai Dahe Chemical Reagent Company. All chemicals were used without further purification.

2.2. Catalyst preparation

The Pt@S1 catalyst was synthesized according to the hydrothermal transformation as described in our previous reports [21]. The mesoporous silica spheres (MSSs, prepared according to Grun et al. [41]) were used as templates and modified with APS at room temperature for 8 h. After the impregnation in the aqueous solution of 0.4 M H₂PtCl₆ for 30 min, the platinum-loaded MSSs (Pt-MSSs) were in situ reduced with 0.01 M KBH₄ aqueous solution and calcined in air at 550 °C for 3 h. Afterward, the particles were seeded with 70 nm silicalite-1 through a layer-by-layer procedure and treated with hydrothermal transformation in the sol with the composition of TPABr:H₂O:NaOH = 18:2000:0.2 for 8 h [42]. The ZMC with Pt-encapsulated was separated by centrifugation and washed with distilled water for three times. To remove the organic ingredients, the obtained samples were calcined in air at 550 °C for 6 h. Finally, a reduction process was adopted in a continuous hydrogen flow at 200 °C to obtain the metallic Pt-encapsulated Pt@S1 catalyst. Some of the as-synthesized Pt@S1 was heavily grinded and used as the reference sample.

2.3. Catalyst characterization

Scanning electronic microscopic (SEM) and energy dispersive spectroscopy (EDS) of the catalysts were recorded on Philips XL30 scanning electron microscope. Transmission electronic microscopic (TEM) images were obtained on JEOL JEM-2010 instrument. The X-ray diffraction (XRD) patterns were tested on a Rigaku

D/MAX-IIA diffractometer over a 2 theta range of 5–80° with Cu K α radiation. The X-ray photoelectron spectroscopy (XPS) analysis was carried out with a Perkin-Elmer PHI 5000C ESCA system using Al K α radiation (1486.6 eV) at a power of 250 W. The pass energy was set at 93.9 eV, and the binding energies (BE) were calibrated by using contaminant carbon at a BE of 284.6 eV. All samples were heavily grinded to expose the Pt species before XPS measurement. The textural properties of the samples were determined from the nitrogen sorption isotherms at –196 °C using a Micromeritics ASAP 2010 system. The elemental analyses were performed by inductively coupled plasma atomic emission spectroscopy (ICP-AES) with the limit of detection 0.001 mg/mL. The solid-state near UV Circular Dichroism (CD) spectra were measured using a MOS-450 (Biologic, France) instrument, with finely grinded KBr powder and a detection range of 200–350 nm.

2.4. Racemization catalytic reaction

The racemization reactions were performed at 70 °C under a hydrogen atmosphere, using 0.1 mmol of S-PEA, 2 mL of toluene and 100 mg of Pt@S1 catalyst for 35 h. The Pt@S1 was isolated by centrifugation and washed with toluene after reaction for further characterizations. The processes were monitored by gas chromatography (GC, HP 5890) with a CP-CHIRASIL-DEX CB chiral column (25 m \times 0.25 μ m, CP7502) and FID detection using decane as an internal standard. The enantiomeric excess (*ee*) of substrate and the selectivity of reaction (*Selec.*) were calculated as follows:

$$ee = \frac{[S-PEA]_t - [R-PEA]_t}{[S-PEA]_t + [R-PEA]_t} \times 100\% \quad (1)$$

$$Selec. = \frac{[R-PEA]_t + [S-PEA]_t}{[S-PEA]_0} \times 100\% \quad (2)$$

2.5. DKR catalytic reaction

Typical DKR reactions were performed under the same condition as above but with 0.1 mmol of rac-PEA, R-PEA or S-PEA as reactants, 50 mg of Novozyme[®] 435 as acylation catalyst and 0.2 mmol of vinyl octanoate as acyl donor. After cooling to room temperature, the catalysts were isolated by centrifugation and washed with toluene for further characterizations and applications. The products were analyzed by the GC as mentioned above, and the by-products were characterized by high-resolution mass spectrometer (HRMS) with a Finnigan MAT 95 (San Jose, CA; USA) double-focusing magnetic sector mass spectrometer.

The conversion of substrate (*Conv.*) as well as *ee*_(product), selectivity (*Selec.*_(product)) and yield of product R-amide were calculated by the Eqs. (3)–(6), respectively.

$$ee_{(product)} = \frac{[Product]_{(R,t)} - [Product]_{(S,t)}}{[Product]_{(R,t)} + [Product]_{(S,t)}} \times 100\% \quad (3)$$

$$Conv. = 1 - \frac{[Substrate]_t}{[Substrate]_0} \times 100\% \quad (4)$$

$$Yield = \frac{[Product]_t}{[Substrate]_0} \times 100\% \quad (5)$$

$$Selec._{(product)} = Yield/Conv. \quad (6)$$

3. Results

3.1. Characterizations of catalysts

Fig. 1 depicts the typical SEM and TEM images of intact-Pt@S1. Obviously, the catalyst shows a uniform spherical morphology

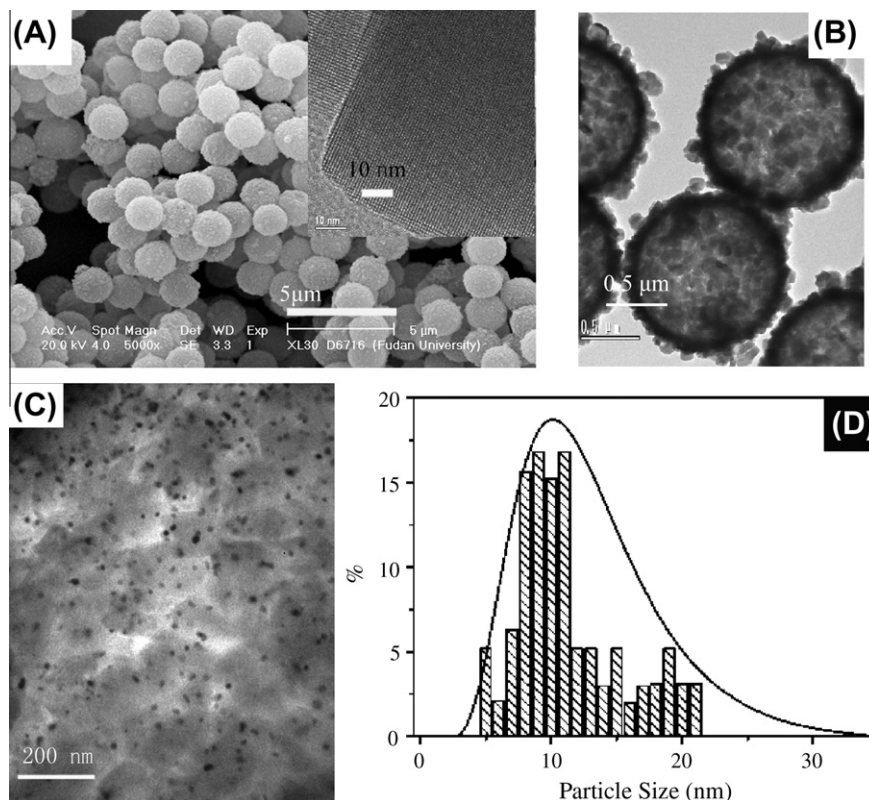


Fig. 1. (A) SEM, (B) TEM and (C) high-resolution TEM images of intact-Pt@S1 and (D) size distribution for the encapsulated Pt nanoparticles. The insets in (A) are the images of zeolitic shell lattice fringes.

(1.6 μm in diameter) with a closely packed silicalite-1 nanocrystal on the surface (Fig. 1A). The lattice of silicalite-1 indicates good crystallinity of the shell, as seen in the inset of Fig. 1A. The hollow interior as well as the dense shell with the thickness of ca. 150 nm can be clearly observed in the TEM image of Fig. 1B. Fig. 1C presents the highly dispersed nanoparticles of Pt inside the capsules. The size distribution of Pt nanoparticles (Fig. 1D, counted with more than one hundred nanoparticles from five pictures of HRTEM of Pt@S1) indicates that they possess a relatively narrow size range with the most probable size of about 10 nm. The platinum content in microcapsule is tested as 3.4 wt% by ICP-AES analysis. The XRD pattern further proves the composition of the intact-Pt@S1, and the sets of peaks attributed to platinum and silicalite-1 are indicated in Fig. 2A-a. To further determine the chemical state of the encapsulated platinum, the XPS operation is conducted after heavily grinding intact-Pt@S1 to expose the Pt component. The binding energies of the Pt 4f band are 71.2 and 74.2 eV (Fig. 2B), respectively, suggesting that platinum in the microcapsule is existed as metallic state [43]. A representative N_2 sorption isotherm and t -plot of intact-Pt@S1 are shown in Fig. 3. The specific surface area calculated by Brunauer–Emmett–Teller (BET) method at P/P_0 of 0.06–0.2 and the micropore volume calculated by t -plot method are 343 m^2/g and 0.1 cm^3/g , respectively, manifesting the good crystallinity and open microporosity of zeolite shell [44].

3.2. The catalytic behavior of Pt@S1 in racemization reaction

The racemization performance of Pt@S1 was first tested in the racemization of S-PEA. As shown in Fig. 4b, the racemization reaction could carry out successfully on Pt@S1 with the selectivity always higher than 99% (Fig. 4d), indicating almost no side reaction occurred in this process. Due to the high selectivity, the ee values of substrate are used directly to express the catalytic

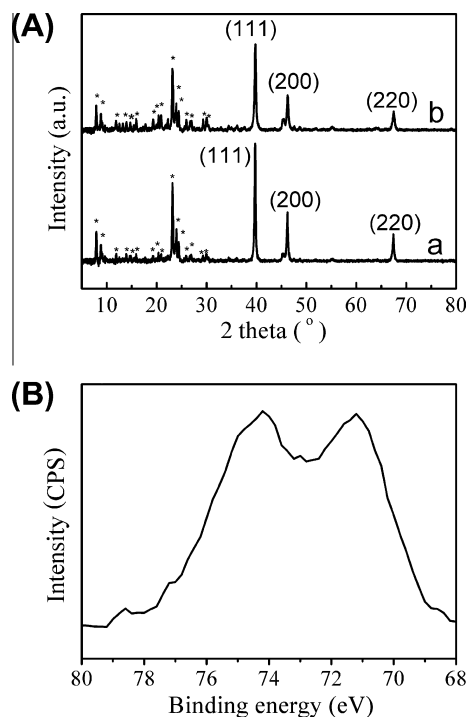


Fig. 2. (A) XRD patterns for intact-Pt@S1 (a) before and (b) after racemization reaction. The characteristic diffractions attributed to zeolite are indicated by *. (B) XPS Pt 4f spectra of grinded Pt@S1.

activity of Pt@S1 for racemization. For comparison, the catalytic performance of broken-Pt@S1 catalyst prepared by heavily

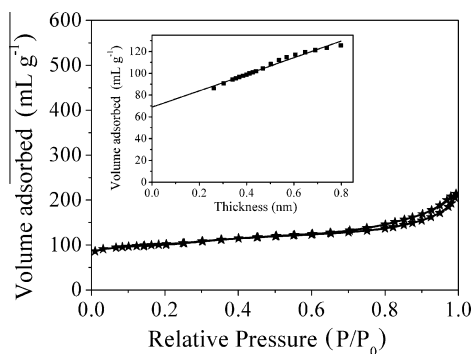


Fig. 3. Representative N_2 sorption isotherm and t -plot (inset) of intact-Pt@S1.

grinding the intact ones is measured under the same conditions, and it is observed that the broken-Pt@S1 catalysts exhibit a similar behavior to intact ones (intact-Pt@S1), illustrating the negligible influence of the zeolitic shell on the diffusion of the reactant (Fig. 4a and b). Besides, compared to that of the fresh intact-Pt@S1 (Fig. 2A-a), the complete maintenance of its XRD diffraction peaks after reaction suggests the high stability of the microcapsular catalyst during the reaction (Fig. 2A-b).

3.3. The catalytic behavior of intact-Pt@S1 in one-pot DKR

The platinum-encapsulated zeolitically microcapsular catalysts (intact-Pt@S1), associated with commercially available Novozyme[®] 435 (intact-Pt@S1/Novozyme[®] 435), were then evaluated in the one-pot DKR of rac-PEA by using vinyl octanoate as acyl donor, and the results were displayed in Fig. 5. It can be clearly found that the whole DKR process for the rac-PEA is able to proceed smoothly with prolonging reaction time. After 35 h, the conversion of rac-PEA and the yield of R-amide could reach up to 80% (Fig. 5b) and 77% (Fig. 5a), respectively. It is worth mentioning that the DKR procedure driven by intact-Pt@S1/Novozyme[®] 435 displays an outstanding selectivity as high as 95% (Fig. 5c) of the target product, and an $ee_{(\text{product})}$ always higher than 99% throughout the whole process.

Fig. 6 further presents the DKR performances of intact-Pt@S1/Novozyme[®] 435 with pure S-PEA or R-PEA as reactants under the same conditions. Both R-PEA and S-PEA exhibit similar tendency to rac-PEA, that is, they also show a high product selectivity (*c.a.*, 95%, Fig. 6c and d) and an increasing conversion with reaction time (Fig. 6a and b). However, the conversion of R-PEA reaches 100% at 25 h, while that of S-PEA just reaches 65% at 35 h, indicating a

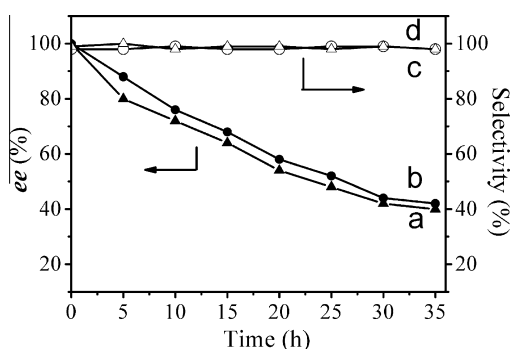


Fig. 4. The (a and b) ee values of substrate and (c and d) reaction selectivity vs reaction time on (a and c) broken-Pt@S1 and (b and d) intact-Pt@S1. The racemization reactions were performed at 70 °C under a hydrogen atmosphere for 35 h, using 0.1 mmol of S-PEA, 2 mL of toluene and 100 mg of catalyst.

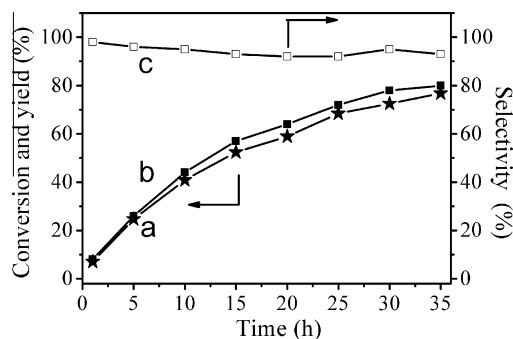


Fig. 5. The (a) yield, (b) conversion and (c) selectivity vs reaction time by using intact-Pt@S1/Novozyme[®] 435 as catalysts. The DKR reaction was performed at 70 °C under hydrogen atmosphere for 35 h, with 0.1 mmol of rac-PEA, 50 mg of Novozyme[®] 435, 0.2 mmol of vinyl octanoate, 2 mL of toluene and 100 mg of intact-Pt@S1.

faster rate for R-PEA than that for S-PEA during the same period, which may be attributed to their different reaction paths as discussed later.

The stability of the intact-Pt@S1/Novozyme[®] 435 catalysts was measured for DKR reaction as well (Table 1). Both catalytic activity and selectivity remain almost unchanged for at least five runs without detectable leaching of Pt, suggesting the good reusability of the ZMC and the enzyme. According to our previous reports [21,22], this promising recycle ability may be attributed to the protection of the zeolitic shell and will be further discussed in Section 4.

3.4. The necessity of the zeolitically microcapsular structure for DKR process

To confirm the necessity of the zeolitic shell on DKR process, the broken-Pt@S1 prepared by heavily grinding the intact-Pt@S1 was also adopted in this procedure with the association of Novozyme[®] 435 (donated as broken-Pt@S1/Novozyme[®] 435). Fig. 7 presents the reaction result of rac-PEA in the system of broken-Pt@S1/Novozyme[®] 435. Its selectivity (Fig. 7c, ~60%) is much lower than that of the intact-Pt@S1/Novozyme[®] 435 catalysts (Fig. 5c, ~95%), although its initial conversion is almost similar to that of the latter. Even worse, after reaction of 10 h, both the conversion and the selectivity for the broken system keep unchanged and remain at only 38% and 61%, respectively, indicating no further reactions occurred after that time. The same behaviors are also observed on both R-PEA and S-PEA. The reactions terminate after

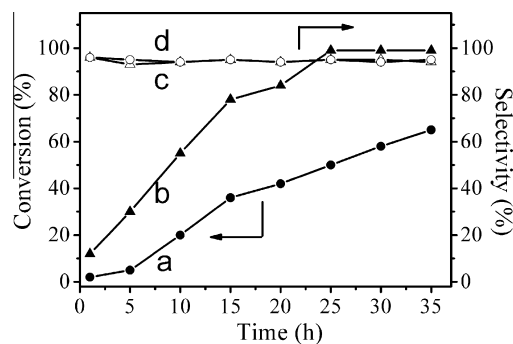


Fig. 6. The DKR (a and b) conversion and (c and d) selectivity of (a and c) S-PEA and (b and d) R-PEA with reaction time by using intact-Pt@S1/Novozyme[®] 435 as catalysts. The DKR reaction was performed at 70 °C under hydrogen atmosphere for 35 h, with 0.1 mmol of S-PEA or R-PEA, 50 mg of Novozyme[®] 435, 0.2 mmol of vinyl octanoate, 2 mL of toluene and 100 mg of intact-Pt@S1.

Table 1
The reusability of intact-Pt@S1/Novozyme®435 in DKR process.

Recycling number ^a	Conv. (%)	Selec. (%)	<i>ee</i> _(product) (%)
1	80	93	>99
2	77	89	>99
3	78	90	>99
4	77	89	>99
5	76	87	>99

^a DKR reaction was performed at 70 °C under hydrogen atmosphere, with 0.1 mmol of rac-PEA, 50 mg of Novozyme®435, 0.2 mmol of vinyl octanoate, 2 mL of toluene and 100 mg of intact-Pt@S1.

10 h (Fig. 8b and c), and the final results of S-PEA (Conv. = 22% and *Selec.*_(product) = 7%, Fig. 8a and b) and R-PEA (Conv. = 42% and *Selec.*_(product) = 70%, Fig. 8c and d) are all much lower than those of intact-Pt@S1/Novozyme®435 (Fig. 6).

4. Discussion

As found in the experimental results, the microcapsular structure is crucial for the good performance of the DKR. The intact-Pt@S1 system with the protection of the intact silicalite-1 shell displays high activity, high selectivity and outstanding reusability, whereas the broken one without the shell protection presents poor results. The scheme 1 illustrates the possible reaction network in our systems. During the process, the rac-PEA would react with an acyl donor through a catalytic acylation process on the enzyme of Novozyme®435. However, the rate of this transformation for R-PEA is much greater than that for S-PEA [45] (proved by the *ee*_(product) > 99%, that is, negligible acylation of S-PEA), and this sharp difference will lead to a concentration gradient of these two enantiomers. Consequently, there is a high tendency for S-PEA to be converted to R-PEA with the assistance of racemization catalyst (Pt@S1 herein), and finally, the optically pure enantiomer can be obtained with an ideal yield of 100%, supposing no by-products generated.

By comparing the proposed scheme with the experimental data, some information could be obtained:

- (1) The highest conversion of intact-Pt@S1/Novozyme®435 for rac-PEA is 80%, while that of broken-Pt@S1/Novozyme®435 is only 38%. According to the mechanism shown in scheme 1, if the Novozyme®435 performs regularly, the conversion of rac-PEA should be 50% in the DKR process even if the racemization catalyst does not work, that is, the R-PEA component is completely acylated. The much lower conversion of

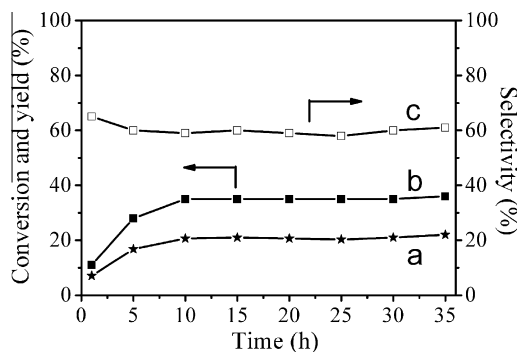


Fig. 7. The (a) yield, (b) conversion and (c) selectivity vs reaction time by using broken-Pt@S1/Novozyme®435 as catalysts. The DKR reaction was performed at 70 °C under hydrogen atmosphere for 35 h, with 0.1 mmol of rac-PEA, 50 mg of Novozyme®435, 0.2 mmol of vinyl octanoate, 2 mL of toluene and 100 mg of broken-Pt@S1.

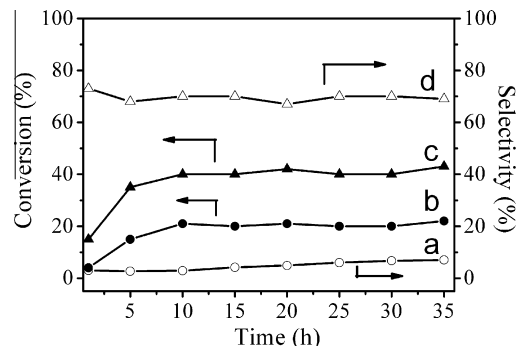
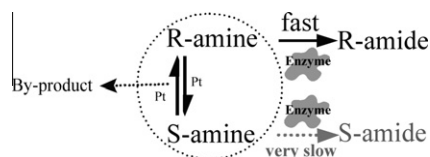


Fig. 8. The DKR (b and c) conversion and (a and d) selectivity of (a and b) S-PEA and (c and d) R-PEA with reaction time by using broken-Pt@S1/Novozyme®435 as catalysts. The DKR reaction was performed at 70 °C under hydrogen atmosphere for 35 h, with 0.1 mmol of S-PEA or R-PEA, 50 mg of Novozyme®435, 0.2 mmol of vinyl octanoate, 2 mL of toluene and 100 mg of broken-Pt@S1.



Scheme 1. The reaction network for the whole DKR process.

the broken system may imply the deactivation of enzyme in this case. The similar conclusion can also be drawn from the experimental results of R-PEA. Its final conversion on intact-Pt@S1/Novozyme®435 can reach 100% after 25 h, while this parameter on broken-Pt@S1/Novozyme®435 is only 42%.

- (2) The intact-Pt@S1/Novozyme®435 with intact shell has a much higher selectivity than the broken one. For example, the selectivity is as high as 95% for rac-PEA on the intact-Pt@S1/Novozyme®435 but that of the broken system is at most 61%. The decrease in selectivity might indicate the occurrence of some side reactions (Scheme 1).
- (3) Theoretically, if the platinum could keep its catalytic activity during the whole reaction process, the conversion of PEA will continuously increase with the reaction time through either racemization reaction or side reactions. However, both the conversion and the selectivity on the microcapsular catalyst with broken shell structure keep unchanged after reaction of 10 h, as shown in Figs. 7 and 8. Such phenomenon means that platinum may also lose its activity for racemization reaction and side reaction when it is exposed in the system.

4.1. Inhibition of zeolitically microcapsular structure for side reactions

To explain the poor selectivity on catalyst without the protection of the zeolite shell, that is, broken-Pt@S1/Novozyme®435, a HRMS experiment was conducted to analyze the products, and one by-product of *N*-ethyl-1-phenylethanamine was identified, which might be generated through the reductive amination process [46]. Referred to the nearly 100% racemization selectivity of broken-Pt@S1 in Fig. 4c, it should be the addition of the vinyl octanoate that causes series of side reactions.

Along with the DKR process, the acyl donor of vinyl octanoate would produce enol-like intermediate and octanoic acid during the reaction. It is known that the vinyl alcohol is unstable in the solution and prefers to undergo the keto-enol tautomerization, leading to the formation of acetaldehyde [46]. Then, the amine in

the system could condense with the acetaldehyde to form the imine via a nucleophilic addition process in the presence of proper acid [46]. Under the atmosphere of hydrogen, reduction in the imine on Pt would give the by-product of *N*-ethyl-1-phenylethan-amine. However, the formation process of imine is greatly dependent on the acidity of the system, since an appropriate acidity has to be provided to give a reasonable concentration of the protonated aldehyde or ketone for the nucleophilic addition reaction [46]. In this system, octanoic acid should be the sole acid source that can promote the side reaction. For the intact-Pt@S1, the more sterically demanding octanoic acid molecules may be difficult to diffuse into the microcapsule due to the space confinement of the micropore on zeolitic shell. As a result, a relatively neutral medium could be formed inside the intact-Pt@S1, limiting the formation of imine. Then, the successive reduction in the imine on Pt in the capsules would become meaningless, ensuring a high selectivity of the DKR. On the other hand, once the microcapsule is crushed, the confined effect of octanoic acid is excluded and the by-product could be easily formed in the open system with the help of octanoic acid, rendering the catalyst with a low selectivity of product.

This explanation of the differences in product selectivity can be validated by three controlled experiments. When octanoic acid or acetaldehyde is added into the DKR system individually instead of vinyl octanoate with the catalyst of only broken-Pt@S1, no by-product could be detected in the reaction system by GC, and the solution is colorless after reaction of 35 h. However, when both octanoic acid and acetaldehyde are synchronously added instead of vinyl octanoate, the solution color changes to light yellow after reaction and the GC analysis shows the formation of by-product. Scheme 2 illustrates these differences of the side reaction paths between intact- and broken-Pt@S1 systems.

The occurrence of side reaction on Pt can also be applied to explain the even worse selectivity for S-PEA than that for R-PEA in the broken-Pt@S1 systems (Fig. 8a and d). As indicated in Scheme 1, when R-PEA is used as reactant, the racemization reaction on Pt and the acylation reaction on Novozyme®435 would occur in parallel. Thus, considerable part of R-PEA would be directly acylated to its corresponding amide, leading to the relative lower possibility of side reactions on Pt. On the contrary, the direct acylation of S-PEA is negligible because of the exclusive stereoselectivity of enzyme.

The substrate has to go through a tandem reaction of racemization on Pt firstly and then acylation on Novozyme®435 to form the final product of R-amide. This process greatly increases the possibility to form the by-products on Pt surface. As a result, the selectivity for S-PEA is lower than that for R-PEA for the broken-Pt@S1.

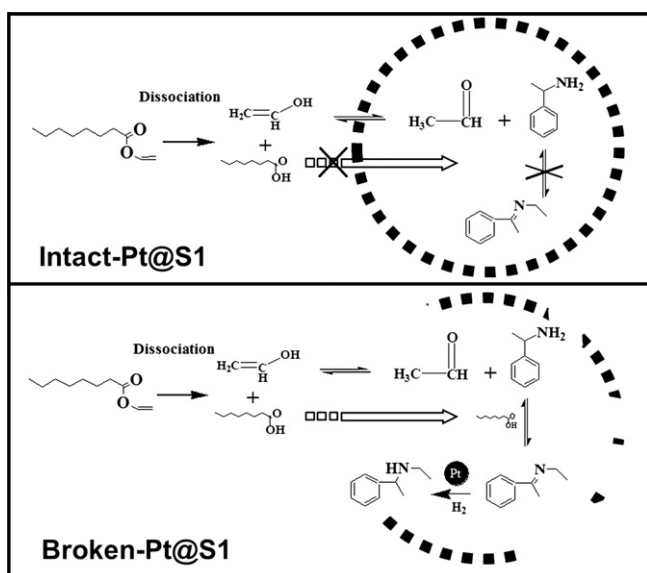
Therefore, the protective zeolitic shell of the intact-Pt@S1/Novozyme®435 functions just as a ‘fence’ that can successfully limit the generation of by-products and ensure the high selectivity of the DKR process for all kinds of enantiomers (Figs. 5 and 6).

4.2. Inhibition of zeolitically microcapsular structure for the deactivation of the catalysts in DKR process

As shown from the experiment results, without the protection of the zeolitic shell, both main and side reactions in DKR process will cease within 10 h and the final conversion and selectivity of substrates on the broken-Pt@S1/Novozyme®435 are all much lower than that with intact ones. According to the mechanism in Scheme 1, they could be attributed to the deactivation of both enzyme and Pt catalysts.

The solid-state near UV circular dichroism (CD) was applied to Novozyme®435 before and after reaction (Fig. 9). The fresh Novozyme®435 presents a CD band at around 270 nm, which is consistent with the literature [47]. This band is almost unchanged in the system involving intact-Pt@S1 after the reaction. However, when the broken-Pt@S1 is applied, the band shifts from 270 nm to 225 nm, illustrating the alteration in the tertiary structure of enzyme [48]. Referring to previous reports, the Pt species in the broken-Pt@S1 can easily leach out from the microcapsule [21,22], and then may migrate to the Novozyme®435 and interact with the N or S atoms in it, leading to the deactivity of the enzyme [49]. Such interaction of Pt with N and S, in turn, will also decrease the activity of Pt species. This migration of Pt species could be experimentally proved by EDS measurement on the Pt@S1 and Novozyme®435. It is found that the intact-Pt@S1 can keep 91% of the original Pt content after reaction, while the broken sample can only keep 18% of Pt comparing to the original catalyst. Correspondingly, the mass ratio of Pt/(C + N + S + Pt) on Novozyme®435 in the intact-Pt@S1/Novozyme®435 system is only 0.1% after reaction, whereas the datum increases to 1.4% when the broken microcapsules are used.

A two-step simulative experiment was further designed to confirm the Pt migrating from broken-Pt@S1 to Novozyme®435 during the DKR process. In step I, only Pt@S1 was put into the reaction system, and in step II, after filtrating out the ZMC, the Novozyme®435 was then added into the solution to trigger the reaction. In this two-step experiment, the racemization and acylation



Scheme 2. The schematic illustration of the inhibition of zeolitically microcapsular structure for the side reactions.

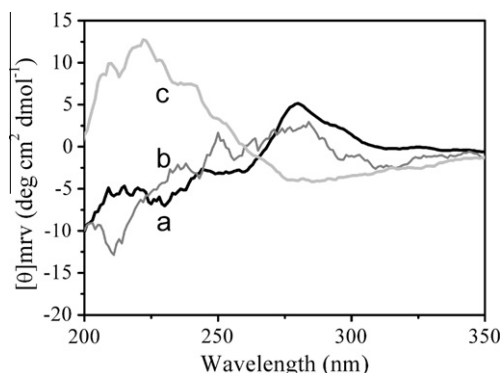


Fig. 9. The solid-state near UV CD spectrum of Novozyme®435 (a) before and after reaction with (b) intact-Pt@S1 and (c) broken-Pt@S1 catalysts.

processes are separated each other, and the transferring of Pt species could be easily monitored by chemical composition analysis. For the convenience of the ICP-AES analysis for solution, an aqueous system is used instead. The Pt concentration in the solution after filtrating intact-Pt@S1 is lower than the limit of detection, while that for broken-Pt@S1 is 1.340 mg/mL, corresponding to 79% of initial Pt content. However, when the fresh Novozyme[®]435 is added in the second step, the Pt concentration in the solution for broken-Pt@S1 dramatically decreases to 0.062 mg/mL, meaning near 95% of Pt has transferred to the Novozyme[®]435. The strong adsorption of Pt on Novozyme[®]435 could also be certified by EDS measurement for broken-Pt@S1, in which the mass ratio of Pt/(C + N + S + Pt) on Novozyme[®]435 isolated after reaction is about 1.3%.

Taking the changes in the CD band of Novozyme[®]435 on different catalysts and the migration of Pt from the broken-Pt@S1 to Novozyme[®]435 into account, it can be concluded that there is a strong interaction between the Pt species and Novozyme[®]435, and such interaction leads to the denaturation of enzyme and the deactivation of Pt. Thus, the reactions terminate in 10 h when the broken-Pt@S1/Novozyme[®]435 is used. For the reaction with intact-Pt@S1/Novozyme[®]435, it is the protection of the zeolitic shell that isolates the Pt and Novozyme[®]435 separately at the inner and outer regions of microcapsule and makes the racemization and acylation reactions get along well with each other. Such protection effect also ensures the high reusability of intact-Pt@S1/Novozyme[®]435 catalyst by preventing the leakage of the Pt and the deactivation of both catalytic components.

4.3. Conversions of different enantiomers

Because of the well synergic catalysis of platinum inside and Novozyme[®]435 outside of the zeolitic shell, the intact-Pt@S1/Novozyme[®]435 system presents promising performance during the DKR of PEA. The catalytic behaviors of various reactants on Pt@S1 can also be well illustrated on the basis of the Scheme 1 and the discussion above.

For intact-Pt@S1, both the Novozyme[®]435 and the platinum could keep their activity well and the one-pot DKR process could proceed successfully. Therefore, the conversion is continuously increasing with high selectivity as the reaction proceeding (Figs. 5 and 6). More interestingly, the increasing rates of conversion with time are different for various amines, that is, R-PEA > rac-PEA > S-PEA. This phenomenon can be well explained by Scheme 1. The R-PEA can be acylated to its corresponding amide directly on Novozyme[®]435 but S-PEA cannot. When the initial contents of total PEA in the three above systems are the same, the initial concentration of the R-PEA is actually different, thus acylation process on the Novozyme[®]435 becomes different. Thereafter, the rates of DKR process are varied during the same period and give rise to various conversions. This difference for the rate of the conversion also appeared for the broken systems during the first 10 h (Figs. 7 and 8), although their conversion and selectivity were much lower than the intact ones. However, since the deactivation of the catalysts took place as indicated above, the conversions for all the systems were remained unchanged finally.

5. Conclusions

In this work, we have explored the feasibility of the ZMC in the DKR process. The intact-Pt@S1/Novozyme[®]435 has been found as a promising catalyst for DKR of PEA, and they display a high selectivity of product with the conversion of 80% as well as a high stability and reusability. The zeolitic shell not only prevents the leakage of

the active Pt species but also prohibits the direct contacting of enzyme with Pt species encapsulated in the ZMC, which ensures the activity and reusability of the catalysts. More importantly, the zeolitic shell provides a protected space that greatly hinders the formation of by-product and gives rise to the higher DKR selectivity. With these advantages, this functional zeolitically microcapsular catalyst may further find applications in the relevant field.

Acknowledgments

This work is supported by NSFC (21073041, 30828010, 20873025 and 20890122), STCSM (10QH1400300, 08DZ2270500 and 09DZ2271400), and 973 and 863 Programs (2009CB930400, 2009CB623506 and 2009AA033701).

References

- [1] C.S. Peyratout, L. Dähne, *Angew. Chem. Int. Ed.* 43 (2004) 3762.
- [2] A.N. Zelikin, Q. Li, F. Caruso, *Angew. Chem. Int. Ed.* 45 (2006) 7743.
- [3] A.F. Faria, R.A. Mignone, M.A. Montenegro, A.Z. Mercadante, C.D. Borsarelli, *J. Agric. Food Chem.* 58 (2010) 8004.
- [4] M. Zandi, S.A. Hashemi, P. Aminayi, *J. Appl. Polym. Sci.* 1 (2011) 586.
- [5] A. Alexeev, R. Verberg, A.C. Balazs, *Langmuir* 23 (2007) 983.
- [6] F. Liu, L.X. Wen, Z.Z. Li, W. Yu, H.Y. Sun, J.F. Chen, *Mater. Res. Bull.* 41 (2006) 2268.
- [7] B. Samanta, X.C. Yang, Y. Ofir, M.H. Park, D. Patra, S.S. Agasti, O.R. Miranda, Z.H. Mo, V.M. Rotello, *Angew. Chem. Int. Ed.* 48 (2009) 5341.
- [8] Y. Zhao, L. Jiang, *Adv. Mater.* 21 (2009) 3621.
- [9] A. Zabet-Khosousi, A.A. Dhirani, *Chem. Rev.* 108 (2008) 4072.
- [10] H.F. Zhang, I. Hussain, M. Brust, M.F. Butler, S.P. Rannard, A.I. Cooper, *Nat. Mater.* 4 (2005) 787.
- [11] A. Corma, *Chem. Rev.* 97 (1997) 2373.
- [12] R.H. Baughman, A.A. Zakhidov, W.A. de Heer, *Science* 297 (2002) 787.
- [13] O. Kreft, A.G. Skirtach, G.B. Sukhorukov, H. Möhwald, *Adv. Mater.* 19 (2007) 3142.
- [14] X.W. Lou, C. Yuan, L.A. Archer, *Adv. Mater.* 19 (2007) 3328.
- [15] J. Wang, H. Zhang, X. Yang, S. Jiang, W. Lv, Z. Jiang, S.Z. Qiao, *Adv. Funct. Mater.* 21 (2011) 971.
- [16] S. Ikeda, S. Ishino, T. Harada, N. Okamoto, T. Sakata, H. Mori, S. Kuwabata, T. Torimoto, M. Matsumura, *Angew. Chem. Int. Ed.* 45 (2006) 7063.
- [17] J. Choi, H.Y. Yang, H.J. Kim, U.S. Son, *Angew. Chem. Int. Ed.* 49 (2010) 7718.
- [18] K. Kamata, Y. Lu, Y. Xia, *J. Am. Chem. Soc.* 125 (2003) 2384.
- [19] D.G. Shchukin, G.B. Sukhorukov, H. Möhwald, *Angew. Chem. Int. Ed.* 42 (2003) 4471.
- [20] G.H. Yang, J.J. He, Y. Zhang, Y. Yoneyama, Y.S. Tan, Y.Z. Han, T. Vitidsant, N. Tsubaki, *Energy Fuels* 22 (2008) 1463.
- [21] N. Ren, Y.H. Yang, J. Shen, Y.H. Zhang, H.L. Xu, Z. Gao, Y. Tang, *J. Catal.* 251 (2007) 182.
- [22] N. Ren, Y.H. Yang, Y.H. Zhang, Q.R. Wang, Y. Tang, *J. Catal.* 246 (2007) 215.
- [23] X. Li, J. He, M. Meng, Y. Yoneyama, N. Tsubaki, *J. Catal.* 265 (2009) 26.
- [24] G. Yang, N. Tsubaki, J. Shamoto, Y. Yoneyama, Y. Zhang, *J. Am. Chem. Soc.* 132 (2010) 8129.
- [25] T.C. Nugent, M. El-Shazly, *Adv. Synth. Catal.* 352 (2010) 753.
- [26] V. Farina, J.T. Reeves, C.H. Senanayake, J.J. Song, *Chem. Rev.* 106 (2006) 2734.
- [27] Y. Kim, J. Park, M.J. Kim, *Tetrahedron Lett.* 51 (2010) 5581.
- [28] D. Koszelewski, B. Grischek, S.M. Glueck, W. Kroutil, K. Faber, *Chem. Eur. J.* 17 (2011) 378.
- [29] M. Breuer, K. Dittrich, T. Habicher, B. Hauer, M. Keßler, R. Stürmer, T. Zelinski, *Angew. Chem. Int. Ed.* 43 (2004) 788.
- [30] C. Ma, X.L. Xu, P. Ai, S.M. Xie, Y.C. Lv, H.Q. Shan, L.M. Yuan, *Chirality* 23 (2011) 379.
- [31] A. Kamal, M.A. Azhar, T. Krishnaji, M.S. Malik, S. Azeeda, *Coord. Chem. Rev.* 252 (2008) 569.
- [32] A. Parvulescu, J. Janssens, J. Vanderleyden, D. De Vos, *Top. Catal.* 53 (2010) 931.
- [33] A. Parvulescu, D. De Vos, P. Jacobs, *Chem. Commun.* 42 (2005) 5307.
- [34] J.S.M. Samec, J.E. Bäckvall, P.G. Andersson, P. Brandt, *Chem. Soc. Rev.* 35 (2006) 237.
- [35] A.N. Parvulescu, P.A. Jacobs, D.E. De Vos, *Chem. Eur. J.* 13 (2007) 2034.
- [36] H.P. Liang, H.M. Zhang, J.S. Hu, Y.G. Guo, L.J. Wan, C.L. Bai, *Angew. Chem. Int. Ed.* 43 (2004) 1540.
- [37] L.G. Hutchins, R.E. Pincock, *J. Org. Chem.* 47 (1982) 607.
- [38] E.J. Ebbers, G.J.A. Ariaans, J.P.M. Houbier, A. Bruggink, B. Zwanenburg, *Tetrahedron* 53 (1997) 9417.
- [39] Y. Govender, T.L. Riddin, M. Gericke, C.G. Whiteley, *J. Nanopart. Res.* 12 (2010) 261.
- [40] B. Martín-Matute, J.-E. Backväll, *Curr. Opin. Chem. Biol.* 11 (2007) 226.
- [41] M. Grun, C. Buchel, D. Kumar, K. Schumacher, B. Bidlingmaier, K.K. Unger, *Stud. Surf. Sci. Catal.* 128 (2000) 155.
- [42] J. Shi, N. Ren, Y.H. Zhang, Y. Tang, *Micropor. Mesopor. Mater.* 132 (2010) 181.

- [43] R. Li, W. Chen, H. Kobayashi, C. Ma, *Green Chem.* 12 (2010) 212.
- [44] A.G. Dong, Y.J. Wang, D.J. Wang, W.L. Yang, Y.H. Zhang, N. Ren, Z. Gao, Y. Tang, *Micropor. Mesopor. Mater.* 64 (2003) 69.
- [45] R. Stürmer, *Angew. Chem. Int. Ed.* 36 (1997) 1173.
- [46] F.A. Carey, *Organic Chemistry*, fourth ed., The McGraw-Hill Companies, United States of America, 2000.
- [47] A. Ganesan, B.D. Moore, S.M. Kelly, N.C. Price, O.J. Rolinski, D.J.S. Birch, I.R. Dunkin, P.J. Halling, *ChemPhysChem* 10 (2009) 1492.
- [48] M.A. Andrade, P. Chacón, J.J. Merelo, F. Morán, *Protein Eng.* 6 (1993) 383.
- [49] J.R. Chang, S.L. Chang, T.B. Lin, *J. Catal.* 169 (1997) 338.